Alkali-Alumina Sorbents for High-Temperature Removal of SO_2

The high-temperature removal of SO_2 by sorbents consisting of sodium and lithium salts supported on α-Al_2O_3 has been investigated with emphasis on the chemistry of regeneration. The sulfated sorbents were regenerated by reduction with CO at 700–800°C in a thermogravimetric analyzer and a packed-bed microreactor. Sulfur removal from the sorbent and distribution of gaseous products were measured at different alkali loadings, temperatures, and CO concentrations. The results are interpreted in terms of a network of reactions wherein alumina is important as a catalyst and as a reactant. During regeneration sulfate is converted to aluminate and sulfide, the fraction of aluminate defining the extent of regeneration. The rate and extent of sulfur removal increase with the ratio of alumina to alkali and are higher in the presence of lithium. The product gas consists of SO_2, COS, and elemental sulfur, the latter compound constituting up to 35% of the sulfur removed.

G. R. Gavalas, Sergio Edelstein, M. Flytzani-Stephanopoulos, T. A. Weston
Department of Chemical Engineering
California Institute of Technology
Pasadena, CA 91125

Introduction

Dry desulfurization of flue gas from coal combustion or sulfide roasting can be carried out using nonregenerable (throwaway) or regenerable sorbents. Limestone and dolomite are essentially the only economical sorbents for throwaway use. These sorbents are employed in calcined form in industrial fluidized boilers and will certainly be utilized when utility fluidized combustion boilers become commercial. Application to pulverized coal boilers is also being investigated in a variety of configurations.

Regenerable sorbents eliminate the extensive solids disposal requirement associated with throwaway sorbents and, under suitable conditions, produce elemental sulfur as a salable byproduct. So far the only regenerable sorbents that have been investigated in some depth are alumina-supported copper oxide (Groenendaal et al., 1976; McCrea et al., 1970; Cho and Lee, 1983) and "alkalized alumina" (Bienstock et al., 1967; Town et al., 1970; Schlesinger and Illig, 1971). Alumina-containing sorbents are also being seriously considered for SO_2 removal in catalytic cracking regenerators (Wall, 1984). Limited effort has been devoted to using calcium-containing materials such as calcium silicates (Yang and Shen, 1979) as regenerable sorbents.

The regeneration of sulfated sorbents requires reduction by hydrogen or carbon monoxide and produces a mixture of gaseous sulfur compounds, including SO_2, COS (or H_2S), and S_2. This off-gas will have to be treated further, e.g., by the Claus process, for final sulfur recovery. The cost of using a regenerable sorbent depends largely on the composition of the off-gas, as well as on the resistance of the sorbent to attrition, especially when used in fluidized reactors.

Among regenerable sorbents, so-called alkalized alumina has been extensively investigated for *in situ* SO_2 removal in fluidized coal combustion (Bienstock et al., 1967; Town et al., 1970; Schlesinger and Illig, 1971). This material is an alkali-deficient sodium aluminate obtained by calcination of sodium aluminum carbonate. Reduction of the sulfated sorbent at 680°C with hydrogen removed over 80% of the sulfur in the form of H_2S. Reduction by carbon monoxide at 680°C produced COS and removed only about 30% of the sulfur in the solid (Schlesinger and Illig, 1971). Successive sulfation-regeneration cycles resulted in sorbent attrition as high as 2.5% per cycle depending on the form of the sorbent and the operating conditions employed. The costs associated with regeneration, final sulfur recovery, and sorbent loss by attrition discouraged further development of this sorbent, at least for application to fluidized combustion.

Instead of using the alkali and alumina components in the form of a homogeneous compound, i.e., sodium aluminate, one can deploy the alkali in supported form, i.e., as a thin film over the pore surface of the alumina. Although at reaction tempera-

Correspondence concerning this paper should be addressed to G. R. Gavalas.
M. Flytzani-Stephanopoulos is now with Department of Chemical Engineering, Massachusetts Institute of Technology, Cambridge, MA 02139.
T. A. Weston is now with E. I. Dupont de Nemours & Co., Wilmington, DE 19898.

tures the two components combine to form aluminate, this compound might be confined to a layer near the pore surface, at least when the alumina employed is of the less reactive alpha form.

The purpose of this work was to investigate sorbents consisting of sodium, lithium, or sodium-lithium mixtures supported on α-Al_2O_3. Sulfur dioxide removal by such sorbents involves the oxidative sulfation

$$M_2O + (SO_2, O_2) \rightarrow M_2SO_4 \quad (1)$$

and the reductive regeneration

$$M_2SO_4 + (CO \text{ or } H_2) \rightarrow M_2O, M_2S + (S_2, SO_2, COS \text{ or } H_2S, CO_2 \text{ or } H_2O) \quad (2)$$

where M is the alkali metal and M_2O represents oxide, carbonate, or aluminate. Sulfation is very rapid and proceeds to completion, but regeneration is complex, involving catalytic and noncatalytic reactions influenced by slow desorption steps. The focus of this work was on elucidating the reaction network and the role of the alkali and alumina components in regeneration.

The results show the profound role of alumina as a reactant and catalyst during regeneration. Increasing the alumina surface area per unit mass of alkali results in faster and more complete regeneration. It is also found that sorbents containing lithium or sodium-lithium mixtures are superior to those containing sodium alone in terms of rate and extent of regeneration. Sulfur is removed as SO_2, COS, and elemental sulfur, S_2. The fraction of elemental sulfur in the sulfur gases decreases with the alkali to alumina ratio and the CO concentration, and decreases with the temperature. Under the conditions of a thermogravimetric analyzer experiment this fraction reached 0.35 with 10% CO. As the concentration of CO is lowered SO_2 and S_2 increase at the cost of COS. When produced in substantial yield, elemental sulfur can be removed by condensation and COS and SO_2 can be recycled to the regeneration stage, obviating the need for further sulfur recovery steps. A conceptual fluidized combustion scheme incorporating this concept has been described by Gavalas et al. (1985). To be economical, the sorbent must possess good resistance to attrition in successive sulfation-regeneration cycles. The present study did not consider the mechanical properties of the sorbents.

Experimental

Sorbents

Table 1 lists the composition of the sorbents investigated. The sorbents were prepared by impregnation of the porous support, which has previously been ground and sieved. One sorbent (NLα2) was also made by impregnation of 4 mm dia. cylinders of α-Al_2O_3. All sorbents except NLα2 and NLα3 were prepared in sulfated form. Those two sorbents were prepared by impregnation with a solution of alkali acetates, followed by calcination at 800°C. The Na_2SO_4/α-Al_2O_3 sorbents were prepared by impregnation either at incipient wetness or in excess solution. All other sorbents were prepared using the incipient wetness technique. Most sorbents were analyzed for sodium and lithium by atomic absorption spectroscopy and some were analyzed for sulfate by barium precipitation. The surface area of a few sorbents was measured by the BET method. Results show little difference in total surface area between sorbent and support material. Typical values are 4–5 m^2/g for α-Al_2O_3 sorbents and 90–100 m^2/g for γ-AL_2O_3 sorbents. At reaction temperatures of 700–800°C, sodium sulfate and lithium sulfate are both solid, while the sodium-lithium sulfate mixture is molten.

Table 1. Composition of Sorbents

Sorbent	Composition	Sorbent Loading	
		mmol M^+/m^2	mg M_2SO_4/g
Nα1	Na_2SO_4/α-Al_2O_3	0.236	83.3
Nα2	Na_2SO_4/α-Al_2O_3	0.476	169.0
Nα3	Na_2SO_4/α-Al_2O_3	0.274	97.3
Nα4	Na_2SO_4/α-Al_2O_3	0.044	15.6
Nγ	Na_2SO_4/γ-Al_2O_3	0.037	235.0
NLα1	$NaLiSO_4/\alpha$-Al_2O_3	0.506	111.2
NLα2	$NaLiSO_4/\alpha$-Al_2O_3	0.435	112.4
NLα3	$NaLiSO_4/\alpha$-Al_2O_3	1.235	319.1
NLγ	$NaLiSO_4/\gamma$-Al_2O_3	0.018	107.3
NLZ	$NaLiSO_4/ZrO_2$	0.112	114.2
NLS	$NaLiSO_4/SiO_2$	0.118	153.0
Lα	Li_2SO_4/α-Al_2O_3	0.373	82.0

Apparatus

Experiments were carried out with a thermogravimetric analyzer (TGA) and a packed-bed reactor. A DuPont 951 thermogravimetric analyzer interfaced to a data acquisition system was used for continuous logging of the weight, the rate of weight change, and the temperature during reaction. The TGA was furnished with a temperature programmer, allowing linear temperature increase or isothermal operation. Gaseous reactants were introduced through a side arm directly into the TGA reaction chamber, while nitrogen diluent flowing through the bulb housing the balance mechanism insured that no corrosive gases would contact the balance mechanism. The flow rates of both gas streams were measured with mass flow meters. The elemental sulfur in the gaseous product was removed by a glass wool filter placed in the exit line of the TGA. The remaining gas phase products were collected by means of a multiport sampling valve and analyzed with a Varian series 3700 gas chromatograph equipped with a flame photometric detector. SO_2 and COS were separated isothermally at 60°C using a Supelco 183 cm × 0.318 cm Chromosil 310 column with a helium carrier flow rate of 30 cm^3/min. Due to the small size of the samples the elemental sulfur produced could not be measured directly.

The other experimental system was a packed-bed reactor consisting of a 0.8 cm ID quartz tube mounted vertically in an electric tube furnace. The sample was held in place by a quartz frit and quartz wool. The temperature of the bed was monitored with a thermocouple inserted within a thermal well imbedded in the solid sample. The flow of reactant gases was measured using calibrated gas flow meters. Elemental sulfur was condensed in traps immersed in an ice bath, and could be measured by weighing. All lines between the reactor and the sulfur traps were heated to prevent condensation of sulfur. Gaseous products were analyzed using a Hewlett-Packard 5750 gas chromatograph equipped with a flame photometric detector and a Supelco 183 cm × 0.318 cm Chromosil 310 column. The column was used isothermally at 60°C with a helium carrier flow rate of 60 cm^3/min.

Procedure

The majority of the experiments involved the reduction of sulfated sorbents, either freshly prepared by impregnation or after one or more cycles of reduction and resulfation. The reducing gas compositions were 2.5% CO–0.15% CO_2, 6% CO–0.3% CO_2, and 10% CO–0.5% CO_2 in N_2. The CO_2 was added in sufficient concentration to prevent carbon deposition. After reduction the sorbents were resulfated using a mixture of 1% SO_2–10% air in N_2.

The sample size in the TGA experiments was 30 to 40 mg. A platinum pan was used for supported-sorbent measurements and a gold-coated platinum crucible was used for a few reference experiments with unsupported alkali salts. The samples were heated to the desired temperature in N_2 and the weight loss during the heating period was monitored to observe any sulfate decomposition. During reduction the weight loss of the sorbent was monitored continuously and gas samples were taken and analyzed for SO_2 and COS. The analysis of each sample required approximately 4 min. At the beginning of the reduction period, the product gas composition was found to change rapidly within the 4 min time span of a gas chromatogram. Therefore samples were initially collected every 15 to 30 s using a multiport valve. During the remainder of the period samples were injected on-line. The collected samples were analyzed at the conclusion of the reduction period.

The sulfur and oxygen contents of the sorbent at the end of a reduction period were determined by measuring the weight gain when the reduced sorbent was exposed to oxygen. All oxygen-deficient sulfur species present were thus oxidized to sulfate. The sorbent was then fully resulfated by exposure to SO_2 and air, and another experiment with different reduction time could be performed. Interpretation of the successive weight changes provides the amount of sulfur, in any form, removed from the sorbent during reduction. Comparison of the total sulfur removed with the total amounts of SO_2 and COS produced, found by integration of gas analysis data, yields the amount of elemental sulfur produced during a reduction period.

For the microreactor experiments 1.5 to 2 g samples were used. As concentrations of the product gas exiting the reactor were at times in excess of those the detector was able to handle, the exit stream was diluted with N_2 prior to injection into the chromatograph. Elemental sulfur collected in the traps was measured gravimetrically after the conclusion of the reduction.

In both the TGA and microreactor experiments the reductions were carried out at 700, 750, or 800°C and at a pressure slightly above atmospheric.

Results

Thermogravimetric experiments

Sulfate and Carbonate Decomposition. Figure 1 shows the standard free energy change for the decomposition of sodium and lithium sulfate and sodium carbonate by reaction with alumina. While the decomposition of the sulfates to form aluminates is highly unfavorable, the carbonate decomposition is favorable at temperatures between 700 and 800°C. In agreement with these predictions, no decomposition of sulfated sorbents supported on α-Al_2O_3 was observed during the sample preheating in a stream of nitrogen. However, all sorbents supported on γ-Al_2O_3 decomposed partially and irreversibly. In each case, decomposition became evident at 450°C and continued with further heating. Sulfation after reduction renewed only the sulfate lost during reduction, but not that lost during heating in nitrogen prior to reduction.

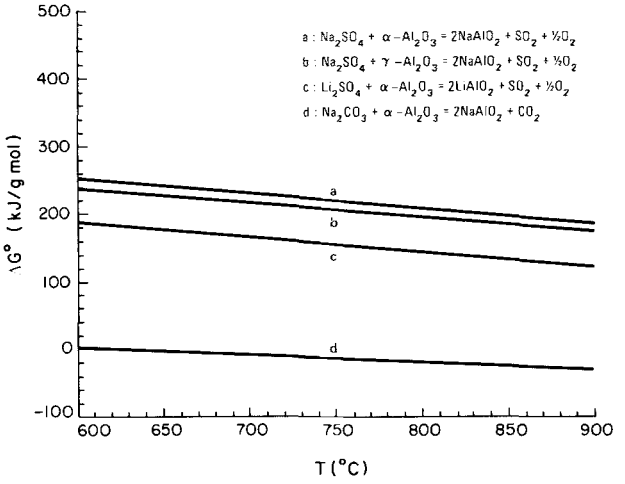

Figure 1. Standard free energy for decomposition of alkali sulfates and carbonate.
Data from JANAF (1971)

The interpretation of the thermogravimetric experiments used to determine the oxygen content of the sorbent requires making a distinction between carbonate and aluminate formed during reduction. To estimate the rate of conversion of carbonate to aluminate, samples of alumina impregnated with various carbonates were heated in the TGA at a constant rate of 100°C/min until reaching 700°C, after which the temperature was held constant at 700°C. The results are shown in Figure 2. In agreement with the equilibrium calculations, sodium-lithium carbonate and lithium carbonate were completely converted at 700°C. The rate of aluminate formation in these cases was comparable to the rate at which carbonate would be formed during reduction. Sodium carbonate begins reaction with alumina between 650 and 700°C. When γ-Al_2O_3 impregnated with sodium-lithium carbonate was heated in N_2, decomposition began at temperatures about 100°C lower than that encountered with α-alumina.

Reduction Experiments. Reduction of a Na_2SO_4/α-Al_2O_3 sorbent (Nα3) at 700 and 800°C with 10% CO yielded the results shown in Figure 3. The weight was adjusted for the amounts of metal present in the sorbent to represent weight loss per initial weight of sulfate. Reduction takes place in two stages at both 700 and 800°C. During the first stage the weight decreases very slowly, with SO_2 as the chief gaseous product. After approximately 1 min at 800°C or 3 min at 700°C, SO_2 is replaced by COS as the major gaseous product, accompanied by an acceleration of the weight loss. This general pattern repeated itself for all sorbents and reaction conditions, both in the TGA and the microreactor. Figure 4 shows similar results for the sorbent containing a sodium-lithium mixture. Under the same temperatures and CO concentrations, the mixed-alkali sorbent is reduced more rapidly than the sorbent containing pure sodium. Figure 5 shows the weight loss curves of sorbents prepared with different alkali loadings. As the alkali loading increases, the reduction rate decreases and the transition from SO_2 to COS production becomes more gradual.

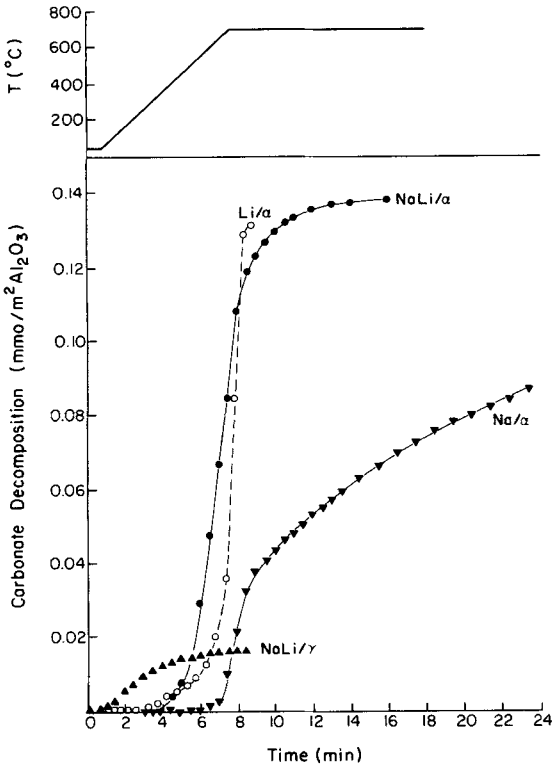

Figure 2. Alkali carbonate decomposition on various supports.

The effect of reductant concentration is depicted in Figure 6. As the CO concentration decreases, the reduction becomes slower and the period of SO_2 production is prolonged. The duration of this period increases dramatically at CO concentrations below 5%, and for 1% CO switchover to COS was not observed.

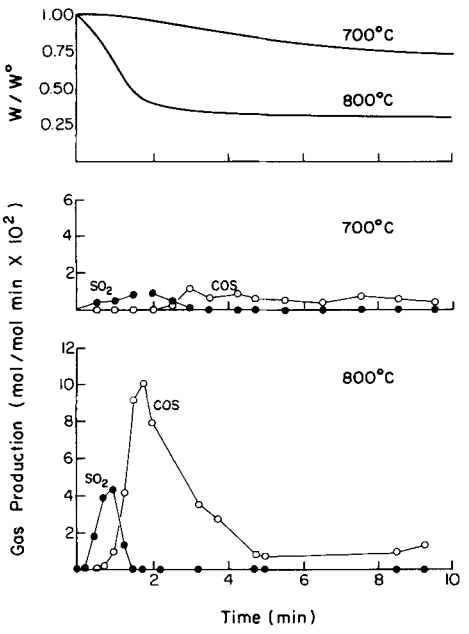

Figure 3. Reduction of Na_2SO_4/α-Al_2O_3 (Nα3) with 10% CO in TGA.
Gas production in mol/initial mol sulfate

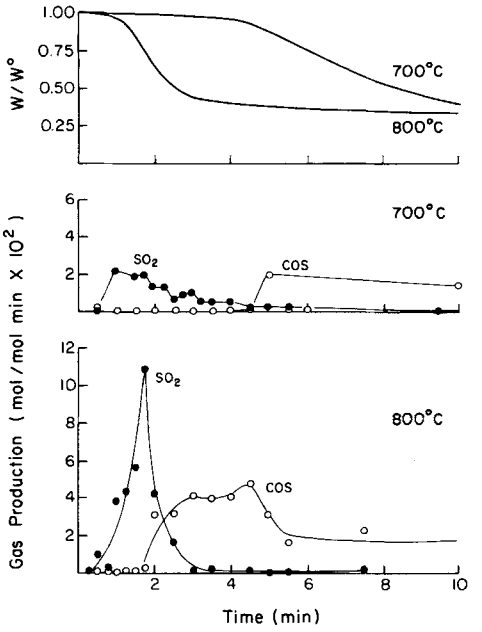

Figure 4. Reduction of $NaLiSO_4/\alpha$-Al_2O_3 (NLα1) with 10% CO in TGA.
Gas production in mol/initial mol sulfate

A longer SO_2 production period was also observed when:

1. α-Al_2O_3 rather than γ-Al_2O_3 was used to prepare the sorbent,
2. Li was one of the alkali constituents
3. The alkali loading was higher
4. The temperature was lower
5. The sorbent had been sulfated at high temperatures prior to reduction.

The cumulative yield of various products after 20 min at 700 and 800°C with 10% CO is shown in Table 2 for several sorbents. Sulfur removal from the sorbent (extent of regeneration) is favored by higher temperature, by using α-Al_2O_3 rather than γ-Al_2O_3, and by using lithium as one of the alkali components. The yield of elemental sulfur in the gaseous products is favored by higher temperature, by using a sodium-lithium mixture

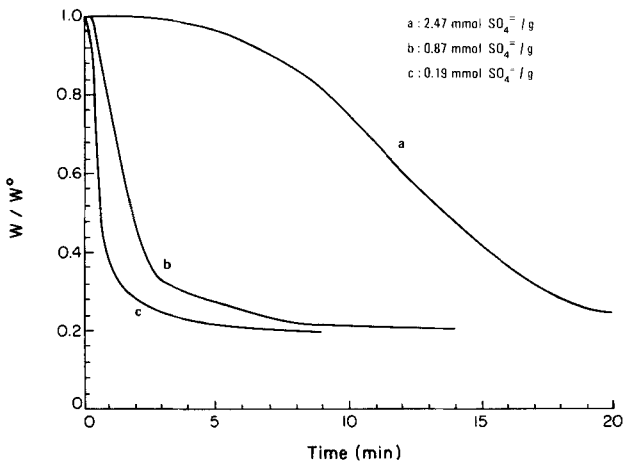

Figure 5. Effect of sorbent loading on reduction of $NaLiSO_4/\alpha$-Al_2O_3 at 800°C with 10% CO in TGA.

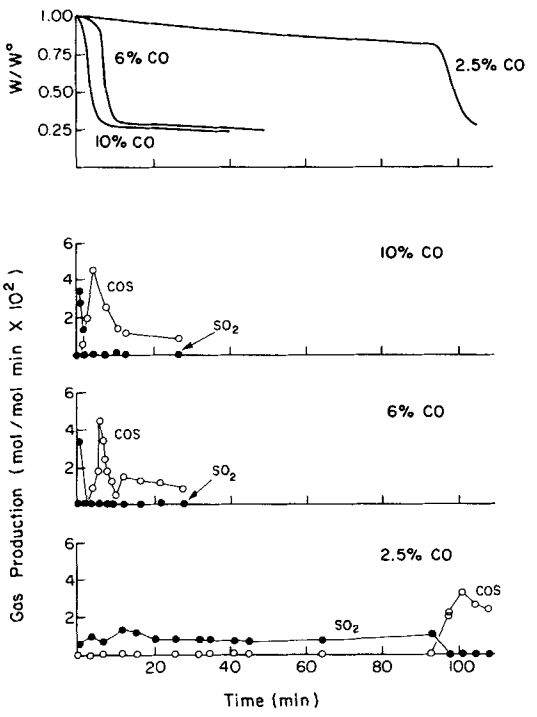

Figure 6. Effect of CO concentration on reduction of $NaLiSO_4/\alpha$-Al_2O_3 (NLα2) at 750°C in TGA.
Gas production in mol/initial Mol sulfate

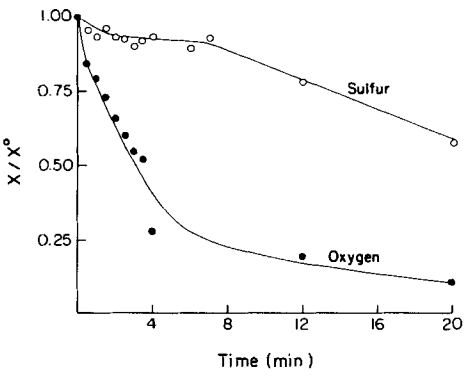

Figure 7. Sorbent elemental composition during reduction of Na_2SO_4/α-Al_2O_3 (Nα1) at 800°C with 10% CO.

rather than sodium or lithium, by using α-Al_2O_3 rather than γ-Al_2O_3, and by decreasing the alkali loading.

Reduction-Oxidation Experiments. The reduction of Na_2SO_4/α-Al_2O_3 and $NaLiSO_4/\alpha$-Al_2O_3 sorbents was examined in greater detail by following sorbent composition as a function of time during reduction. By interrupting the reduction at different times and measuring the weight increase associated with oxidation in air and subsequent exposure to SO_2 and air, the total sulfur and total oxygen in the sorbent could be determined as discussed earlier. The results of the reduction at 800°C with 10% CO of a Na_2SO_4/α-Al_2O_3 sorbent and of a $NaLiSO_4/\alpha$-Al_2O_3 sorbent are shown in Figures 7 and 8, respectively. During the first stage of reduction oxygen is removed from the sorbent at a higher rate than is sulfur. During the second stage, the oxygen content remains almost constant while sulfur continues to decline at a substantial rate. Differences in the reduction of the two sorbents are more prominent in the initial period, during which the sulfur content of the sodium-lithium sorbent, Figure 8, decreases to a much greater extent than that of the sodium sorbent, Figure 7. The rate of sulfur loss during the second half of the reduction appears to be approximately the same for both sorbents. At 700°C similar variations between the two sorbents are exhibited, but sulfur removal during the later period is much slower than at 800°C.

Microreactor experiments

Sorbents with various alkali components and supports were reduced at different temperatures and CO concentrations using the microreactor system. Gas production exhibited behavior similar to that in the TGA experiments in that the major gas product switched from SO_2 to COS, the switchover time varying with reaction conditions. Significant amounts of elemental sulfur were produced during the nitrogen purge that followed the reduction.

Sorbents containing lithium-sodium mixtures supported on

Table 2. Product Selectivity after 20 min Reduction with 10% CO in the TGA

Sorbent (Alkali Loading) mmol M^+/m^2		T °C	S in Sorbent	$\frac{S}{S + COS + SO_2}$	$\frac{COS}{S + COS + SO_2}$	$\frac{SO_2}{S + COS + SO_2}$
Nα3	(0.274)	800	0.620	0.224	0.701	0.075
Nα3	(0.274)	700	0.934	0	0.726	0.274
Nα4	(0.044)	800	0.115	0.305	0.502	0.193
Nα4	(0.044)	700	0.802	0	0.727	0.273
NLα1	(0.506)	800	0.285	0.351	0.497	0.152
NLα1	(0.506)	700	0.426	0.082	0.730	0.188
NLα2	(0.435)	800	0.214	0.240	0.585	0.174
NLα3	(1.235)	800	0.311	0.080	0.561	0.358
Lα	(0.373)	800	0.216	0.271	0.630	0.098
Lα	(0.373)	700	0.560	0	0.885	0.115
Nγ	(0.037)	800	0.687	0.079	0.748	0.173
Nγ	(0.037)	700	0.902	0	0.612	0.388
NLγ	(0.018)	800	0.730	0	0.452	0.548
NLγ	(0.018)	700	0.876	0	0.516	0.484

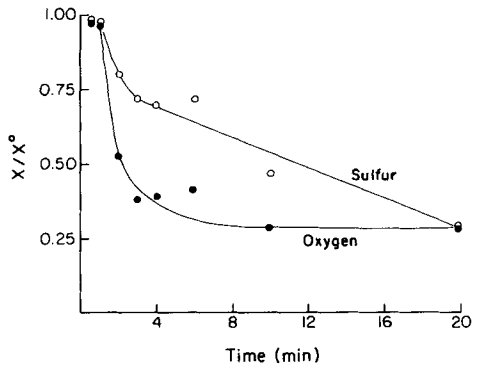

Figure 8. Sorbent elemental composition during reduction of $NaLiSO_4/\alpha$-Al_2O_3 (NLα1) at 800°C with 10% CO.

SiO_2 and ZrO_2 were also studied in the microreactor. SO_2 was the major gas product during the entire reduction of the silica sorbent. Very little sulfur was produced during the N_2 purge and, more important, the reduced sorbent was unable to reabsorb SO_2, thus making silica an unacceptable support. ZrO_2 on the other hand exhibited a pattern similar to that of α-alumina.

Infrared spectrometry

Samples were prepared by reduction in the TGA for the desired length of time, cooling in nitrogen, grinding, and forming a mull that was pressed between KBr windows. Fourier-transform infrared spectrometry (FTIR) was carried out on a Mattson Sirius 100 instrument using a TGS detector. Each spectrum was generated by averaging 512 scans in the range 400–4,000 cm^{-1}. The spectra were reduced by subtraction of the spectrum of the alumina substrate and the reduced spectra was compared to known absorption bands (Weston, 1985). Shifting baselines and variations in mull preparation caused difficulty in extracting quantitative information. In view of the large fraction of alumina in the sorbent (approximately 90%), and the strong absorption of alumina in the spectral region below 900 cm^{-1}, the spectra contained useful information mainly in the region above 900 cm^{-1}. A typical series of spectra for sorbent NLα1 ($NaLiSO_4/\alpha$—Al_2O_3) reduced for different periods is shown in Figure 9. The region above 900 cm^{-1} contains strong absorption bands for SO_4^{2-} around 1,150 cm^{-1}. An SO_3^{2-} band around 980 cm^{-1} appears in the 1 min sample but is absent from the other samples.

Discussion

Background information

In this section we first review thermodynamic data and experimental results from the literature useful to the interpretation of our results.

Homogeneous Reactions. Figure 10 shows the free energy of various reduction reactions. While reduction of sulfate to sulfite is marginally feasible, reduction of sulfate or sulfite to sulfide is highly favorable thermodynamically. In previous work reduction of bulk (unsupported) sodium sulfate by CO at 900°C gave a mixture of sulfide, carbonate, and smaller amounts of polysulfides (Ahlgren et al., 1967). The reaction time was on the order of 1 h under mass-transfer-limited conditions. Sodium sulfate dissolved in molten sodium carbonate was reduced with H_2 and

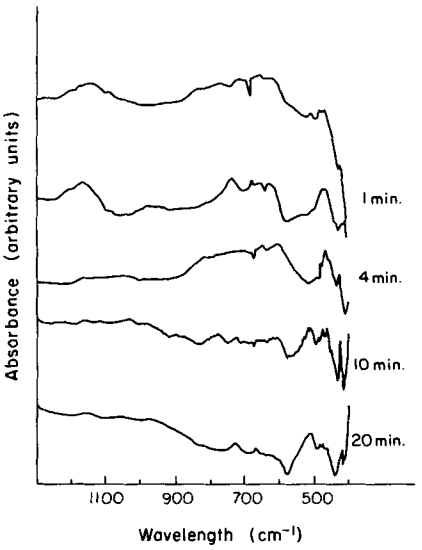

Figure 9. Infrared absorption spectra of $NaLiSO_4/\alpha$-Al_2O_3 (NLα1) reduced at 800°C with 10% CO for various times.

CO at 600 to 840°C, also producing sulfide and possibly polysulfides (Oldenkamp and Margolin, 1969; Birk et al., 1971). The reaction time was on the order of 1 h at 840°C and 6 h at 700°C. Reduction with hydrogen was approximately three times faster than reaction with carbon monoxide.

Although sulfite has not been identified in these previous studies, it is a likely intermediate in sulfate reduction. This compound could then be reduced further or disproportionated. An early study of sulfite disproportionation (Foerster and Kubel, 1924) showed conversion to sulfate and sulfide according to the stoichiometric reaction

$$4Na_2SO_3 = Na_2S + 3Na_2SO_4 \qquad (3)$$

with reaction time on the order of 0.5 h at 700°C. In the presence of SiO_2, sodium sulfite formed sodium silicate, with the release of SO_2 (Manring et al., 1967). Reactions of sodium sul-

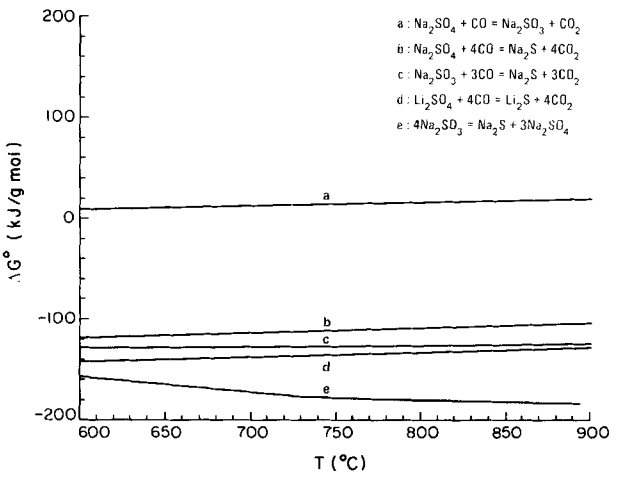

Figure 10. Standard free energy for reduction of alkali sulfate to sulfite and sulfide.
Data from JANAF (1971)

fide and sodium sulfite dissolved in the ternary eutectic Na_2SO_4—K_2SO_4—$LiSO_4$ were studied at 600°C by Dearnaley et al. (1983). The disproportionation of sulfite in this eutectic followed the stoichiometry of reaction 3, but the rates were significantly higher than for the pure sulfite. Disproportionation of sulfite in the presence of SO_2 produced sulfate (but not sulfide) and elemental sulfur. The measured product distribution was explained by the reactions

$$SO_2 + 2SO_3^{2-} = \tfrac{1}{2} S_2 + 2SO_4^{2-} \quad (4)$$

$$2SO_2 + S^{2-} = S_2 + SO_4^{2-} \quad (5)$$

Under the conditions used in our TGA experiments, the reduction of unsupported sulfate would follow the sequence

$$SO_4^{2-} + CO = SO_3^{2-} + CO_2 \quad (6)$$

$$4SO_3^{2-} = S^{2-} + 3SO_4^{2-} \quad (7)$$

leading to sulfide as the final product. Direct reduction of sulfite to sulfide,

$$SO_3^{2-} + 3CO = S^{2-} + 3CO_2 \quad (8)$$

is favorable thermodynamically, as shown in Figure 10, but has not been studied directly.

Heterogeneous Reactions. In the presence of alumina, the sulfite formed by Eq. 6 could decompose by the reaction

$$SO_3^{2-} + Al_2O_3 = SO_2 + 2AlO_2^- \quad (9)$$

Figure 11 shows the Gibbs free energy of the reaction between sodium sulfite and alumina with SO_2 produced in the gas phase. The Gibbs free energy of reaction 9 would be substantially more negative if SO_2 were produced in chemisorbed form. In the presence of CO_2, sulfite could be converted to carbonate, which in turn could form aluminate,

$$SO_3^{2-} + CO_2 = SO_2 + CO_3^{2-} \quad (10)$$

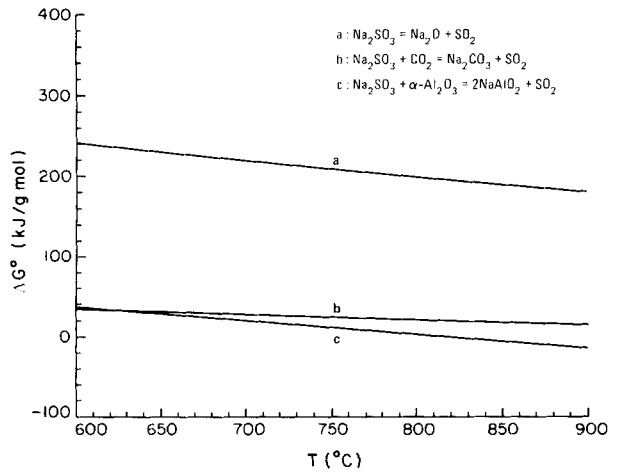

Figure 11. Standard free energy for decomposition of sodium sulfite.
Data from JANAF (1971)

$$CO_3^{2-} + Al_2O_3 = CO_2 + 2AlO_2^- \quad (11)$$

Relevant equilibria are listed in Figures 1 and 11.

The sulfur dioxide produced by reaction 9 reacts further with carbon monoxide to form elemental sulfur and carbonyl sulfide according to

$$SO_2 + 2CO = \tfrac{1}{2} S_2 + 2CO_2 \quad (12)$$

$$\tfrac{1}{2} S_2 + CO = COS \quad (13)$$

Khalafalla and Haas (1972) studied the mechanism of reaction 12 catalyzed by γ-Al_2O_3 at temperatures of 450–600°C and suggested chemisorption of SO_2 on Brönsted sites as the first step. They also found that elemental sulfur formed on the alumina surface accelerates the reaction rate. In a series of experiments performed in our laboratory it was found that α-Al_2O_3 and α-Al_2O_3 impregnated with sodium carbonate catalyzed reaction 12 at 700–800°C, producing a mixture of COS and S_2 (Weston, 1985). At 800°C the product composition was at equilibrium according to reaction 12. Evidently, Brönsted sites are not essential at temperatures above 700°C, for α-Al_2O_3 and aluminate do not contain such sites. The formation of COS from CO and S_2, reaction 13, and its reverse are known to be catalyzed by several refractory oxides such as Al_2O_3 and SiO_2 (Haas and Khalafalla, 1973; Akimoto et al., 1984).

With the above background information we proceed to interpret the two distinct periods in sulfate reduction experiments.

Sulfate reduction

For all sorbents and experimental conditions employed the reduction progressed in two stages, the first characterized by SO_2 release, the second by COS and S_2 release, Figures 3, 4, and 6. Comparison of Figures 3 and 7 and Figures 4 and 8 shows that the stage of SO_2 production is also characterized by fast removal of oxygen and slow removal of sulfur from the sorbent. During the stage of COS production, the removal of oxygen slows while that of sulfur accelerates. Removal of sulfur during the first stage is solely in the form of SO_2, while removal during the second stage involves release of S_2 as well as COS. The release of S_2 during the second stage is inferred from the TGA measurements by comparison of COS release and sulfur removal.

The product SO_2 during the first stage of reduction derives from reactions 6 and 9 in sequence, where reaction 6 is catalyzed by the alumina surface. Part of the SO_2 produced escapes to the gas phase, the other part remains chemisorbed subject to further reduction by reactions 12 and 13. The sulfite produced by reaction 6 reacts with alumina, reaction 9, or disproportionates by the homogeneous reaction 7. Sulfur dioxide production during reduction of unsupported sulfate was observed to be negligible.

The switching from SO_2 production to COS and S_2 production cannot be explained solely by the consecutive nature of reactions 9 and 12, for COS production is essentially zero during the first stage. One possible explanation is the activation of reaction 12 by the elemental sulfur buildup on the surface, as reported by Khalafalla and Haas (1972) for catalysis by γ-Al_2O_3 at lower temperatures. Another possible explanation is offered by the reaction of S_2 or COS with the remaining sulfate to yield sulfite or sulfide and SO_2, e.g.,

$$\tfrac{1}{2} S_2 + 2SO_4^{2-} = 2SO_3^{2-} + SO_2 \quad (14)$$

$$S_2 + SO_4^{2-} = 2SO_2 + S^{2-} \qquad (15)$$

Similar reactions could take place between COS and SO_4^{2-}. Assuming these reactions to be sufficiently rapid, no S_2 or COS could be released until all sulfate has been consumed.

This second explanation of the separate evolution of SO_2 and COS is supported by the infrared spectra of sorbent samples corresponding to different reduction times. Figure 9 shows that the sulfate band declines relatively rapidly and disappears altogether in less than 4 min. A sulfite band, absent from the fresh sulfated sorbent, appears after 1 min but again disappears within 4 min reduction time. The time required for disappearance of the sulfate ion is comparable to the time of changeover from SO_2 to COS production, consistent with the explanation based on reactions 14 and 15. The changeover time also increases with alkali loading, providing further evidence in favor of reactions 14 and 15, inasmuch as the time for elemental sulfur buildup required for acceleration of reaction 12 would be independent of alkali loading.

The carbonyl sulfide released during the second stage could arise from the reaction of CO with elemental sulfur, reaction 13, or from the reaction of CO_2 with the sulfide ion,

$$S^{2-} + CO_2 + Al_2O_3 = 2AlO_2^- + COS \qquad (16)$$

Figure 12 shows the free energy of reaction 16 for sodium sulfide and lithium sulfide. To explore the role of reaction 16, an experiment was performed in the TGA wherein the reactant gas was switched from CO to CO_2 at the onset of the COS production stage in the TGA. The weight curve obtained is compared with the uninterrupted reduction of the same sorbent in Figure 13. When CO_2 is introduced in the system, the production of COS ceases completely and the major gas product changes to SO_2. The reaction responsible for this product is

$$\tfrac{1}{2}S_2 + 2CO_2 = SO_2 + 2CO \qquad (17)$$

which in spite of a standard free energy of +92 kJ/gmol at 800°C would proceed in the presence of 10% CO_2 and very low concentrations of CO. The elemental sulfur participating in this reaction could derive from chemisorbed sulfur produced earlier

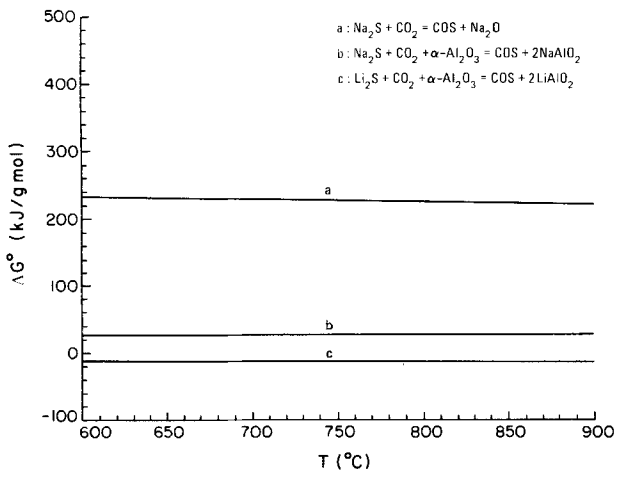

Figure 12. Standard free energy for reaction between alkali sulfide and CO_2.
Data from JANAF (1971)

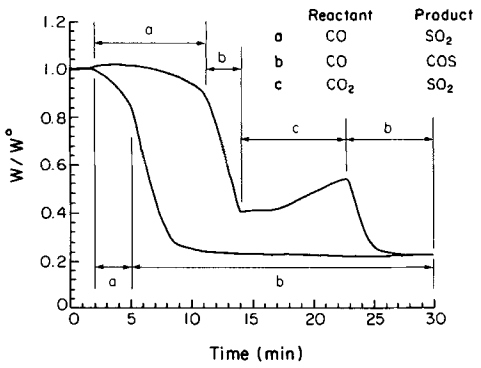

Figure 13. Effect of CO_2 on weight loss and gas production during reduction of a $NaLiSO_4/\alpha\text{-}Al_2O_3$ sorbent (NLα2) at 750°C with 5% CO.

or from sulfide via reaction 16a, below. In the presence of large amounts of CO_2 and the absence of CO the latter reaction would produce S_2 rather than COS and carbonate rather than aluminate,

$$S^{2-} + 2CO_2 = CO_3^{2-} + CO + \tfrac{1}{2}S_2 \qquad (16a)$$

so that the stoichiometric result of reactions 16a and 17 would be

$$S^{2-} + 4CO_2 = CO_3^{2-} + 3CO + SO_2 \qquad (18)$$

The weight increase observed in section *c* of Figure 13 is due to this carbonate formation as well as to aluminate conversion to carbonate in the presence of carbon dioxide.

The long tail in the rate of COS production in Figures 3 and 4 is probably due to the slow kinetics of reaction 16, in view of the low concentration of CO_2 in the reactant gas. Figure 14 assembles the various reactions discussed above into a highly coupled reaction network.

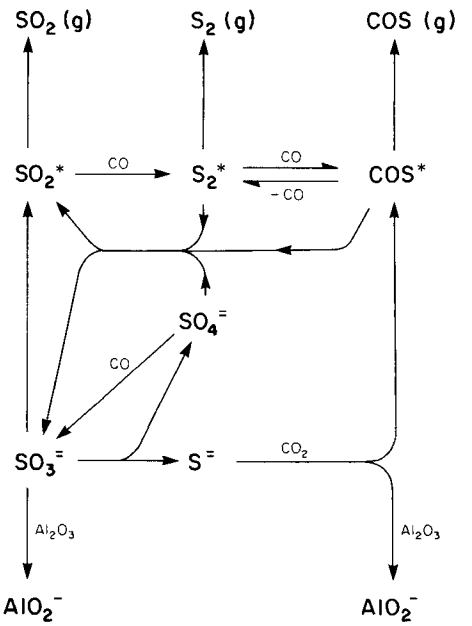

Figure 14. Proposed reaction network.
*chemisorbed species

Effects of alkali loading and operating conditions

The effect of alkali loading is shown in Figure 5 and Table 2. As shown in Figure 5, the rate of weight loss increases markedly with decreasing alkali loading, i.e., with increasing surface area of alumina per unit mass of alkali. This effect of alumina is clearly due to the direct reaction 9 as well as to the catalytic reactions 12 and 13. Table 2 shows that sulfur removal at fixed temperature and reaction time increases with decreasing alkali loading, the effect being more pronounced for the mixed-alkali sorbents. These effects are explained by the competition between the homogeneous sulfite disproportionation, reaction 7, and reaction 9 and subsequent surface catalyzed reactions 12, 13, and 16.

At fixed alkali loading the pure lithium and sodium-lithium sorbents undergo faster reduction and more extensive sulfur removal than the pure sodium sorbent. This effect may be due to the faster reaction 9 in the presence of the counterion Li^+. Evidence for the increased reactivity of lithium salts in aluminate formation is offered by the results of Figure 2, concerning the carbonate-alumina reaction.

Temperature has a strong effect on the reaction rate, Figures 3 and 4, and the product distribution. In particular, the ratio of elemental sulfur to the total sulfur removed during reduction in the TGA is zero at 700°C and 0.2–0.4 at 800°C. In the microreactor experiments, elemental sulfur production at 700°C was zero during reduction but substantial during subsequent purge by nitrogen. Measurements of sulfur chemisorption currently under way show that elemental sulfur is very strongly chemisorbed on α-Al_2O_3 (e.g., desorption time at 700°C is on the order of 5 h).

The concentration of carbon monoxide has a strong effect on the rate of weight loss and product distribution. Figure 6 shows the reaction time increasing twentyfold as the CO concentration is reduced from 10 to 2.5%. At the 2% CO level, the shift from SO_2 to COS is greatly delayed and the SO_2 yield is much higher. Similar trends were observed in the packed bed reactor runs where decreasing the concentration of CO from 10 to 1% increased the yield of SO_2 and elemental sulfur at the cost of COS.

Acknowledgement

This work was supported by the National Science Foundation, Grant No. CPE-8121892.

Literature cited

Ahlgren, P., S. Lemon, and A. Leder, "Preparation of Sodium Polysulfides by Solid and Molten State Reactions," *Acta Chem. Scand.*, **21,** 1119 (1967).

Akimoto, M., K. Yamagami, and E. Echigoya, "A Mechanistic Study on Vapor-Phase Catalytic Oxidative Dehydrogenation of Ethylbenzene with Carbonyl Sulfide," *J. Catal.*, **86,** 205 (1984).

Bienstock, D., J. H. Field, and J. G. Myers, U.S. Bureau of Mines Rep. Inv. No. 7021 (1967).

Birk, J. R., C. M. Larsen, W. G. Vaux, and R. D. Oldenkamp, "Hydrogen Reduction of Alkali Sulfate," *Ind. Eng. Chem. Process Des. Develop.*, **10**(1), 7 (1971).

Cho, M. H., and W. K. Lee, "SO_2 Removal by CuO on γ-Alumina," *J. Chem. Eng. Japan,* **16**(2), 127 (1983).

Dearnaley, R. I., D. H. Kerridge, and D. J. Rogers, "Molten Lithium Sulfate-Sodium Sulfate-Potassium Sulfate Eutectic: Reactions of Some Sulfur Compounds," *Inorg. Chem.*, **22,** 3242 (1983).

Foerster, V. F., and K. Kubel, "Uber die Zerstezung der Schwefligsauren Salze in der Gluhhitze," *Z. Anorg. Allge. Chem.*, **139,** 261 (1924).

Gavalas, G. R., T. A. Weston, and M. F. Stephanopoulos, "Alkali-Alumina Sorbents for Regenerable SO_2 Removal in Fluidized Coal Combustion," 8th Int. Conf. Fluidized Combustion, Houston (Mar., 1985).

Groenendaal, W., J. E. Naber and J. B. Pohlenz, "The Shell Flue Gas Desulfurization Process: Demonstration on Oil and Coal Fired Boilers," *AIChE Symp. Ser.*, **72**(156) 12 (1976).

Haas, L. A., and S. E. Khalafalla, "Catalytic Thermal Decomposition of Carbonyl Sulfide and Its Reactions with Sulfur Dioxide," *J. Catal.*, **30,** 451 (1973).

JANAF Thermochemical Tables, 2nd ed., NSRDS-NS-37 (1971).

Khalafalla, S. E., E. F. Foerster, and L. A. Haas, "Catalytic Reduction of Sulfur Dioxide on Iron-Alumina Bifunctional Catalysts," *Ind. Eng. Chem. Prod. Res. Develop.*, **10**(2), 133 (1971).

Khalafalla, S. E., and L. A. Haas, "Active Sites for Catalytic Reduction of SO_2 with CO on Alumina," *J. Catal.*, **24,** 115 (1972).

Manring, W. H., D. D. Billings, A. R. Conroy, and W. C. Bauer, "Reduced Sulfur Compounds," *Glass Industry,* 374 (1967).

McCrea, D. H., A. J. Forney, and J. G. Myers, *J. Air Pollut. Control Assoc.*, **20**(12), 819 (1970).

Oldenkamp, R. D. and E. D. Margolin, "The Molten Carbonate Process for Sulfur Oxide Emissions," *Chem. Eng. Prog.*, **65**(11), 73 (1969).

Schlesinger, M. D., and E. G. Illig, "The Regeneration of Alkalized Alumina," *Chem. Eng. Prog. Symp. Ser.*, **67**(115), 46 (1971).

Town, J. W., J. I. Paige, and J. H. Russell, "Sorption of Sulfur Dioxide by Alkalized Alumina in a Fluidized-Bed Reactor," *Chem. Eng. Prog. Symp. Ser.*, **66**(105), 260 (1970).

Wall, J. D., "Control FCC SO_x Emissions," *Hydrocarbon Processing,* **45,** (Oct., 1984).

Weston, T. A., "The Regeneration of High-Temperature Sulfur Dioxide Sorbents: The CO Reduction of Supported Alkali Sulfates," Ph.D. Diss. California Inst. Tech. (1985).

Yang, R. T., and M. S. Shen, "Calcium Silicates: A New Class of Highly Regenerative Sorbents for Hot Gas Desulfurization," *AIChE J.*, **25,** 5 (1979).

Manuscript received Feb. 24, 1986, and revision received June 20, 1986.